PULSE CONTROL IN AN ACCELERATOR FOR HEAVY-ION FUSION*

W. M. Sharp, J. J. Barnard, and S. S. Yu[(a)]
Lawrence Livermore National Laboratory, University of California
Livermore, California 94550

Abstract

In induction accelerators proposed for heavy-ion fusion, the ion beam is usually confined longitudinally by an axial electric field tailored to balance the space-charge field. Since generating such electric field "ears" is costly and imprecise, it is important to know how frequently the ears must be applied and what errors in the waveform are tolerable. For practical parameters, cell breakdown is found to impose the principal limit on the spacing of the acceleration modules applying the ear field. Also, it is demonstrated that ear fields may be approximated in several ways by discrete field steps with little impairment of the longitudinal confinement.

I. Introduction

Unlike radio-frequency accelerators, induction accelerators normally provide no longitudinal confinement of a beam. Consequently, in applications, such as drivers for heavy-ion fusion (HIF), that require high current densities, induction accelerators must provide auxiliary confinement to prevent unacceptable lengthening of pulses during acceleration. The usual method proposed for longitudinal confinement is to apply appropriately chosen electric-field spikes at the beam ends that balance the space-charge force by slowing the beam head and accelerating the tail. To exactly balance space charge, these field "ears" would have to be applied continually, and it is shown later that the required ear field in that case would be

$$E_{ear} \approx -g \frac{\partial}{\partial \tau} \left(\frac{I_b}{\beta^2 c^2} \right), \tag{1}$$

where I_b is the beam current, βc is the beam axial velocity, τ is the time a beam slice arrives at some specified position s along the accelerator, and g is an inductance-like factor depending on the beam geometry. In fact, the ear field is only expected to be applied in selected induction modules, referred to here as "ear cells". If the ear field is applied only across cell gaps with a total length L_g in a lattice of N periods, than the field in Eq. (1) must be increased by a factor of $2NL/L_g$, where L is the half-lattice period.

The two methods have been suggested for generating ear fields. Pulse-forming lines (PFLs), which are transmission lines "tuned" by lumped circuit elements, give an accelerating field with a smooth time variation, but they offer limited control over the pulse shape. Due to the finite response time of the circuite elements, the output signal of a PFL typically cuts off the high-frequency components of the desired signal. Also, since PFLs either synthesize the ear voltage as part of a periodic waveform or obtain it by differentiating a square pulse, this approach is quite inefficient. A more flexible and efficient method for generating ear fields is to use banks of field-effect transistors (FETs). A group of FETs can be switched in series to generate a voltage step, and the output of many such banks, appropriately staggered in time, can be combined in an inductive adder to produce a staircase approximation to the ideal ear voltage. Since FET-controlled pulsers are much more costly than ordinary induction pulsers, it is important to know how frequently the ear fields must be applied to be effective. Also, effects of using a staircase approximation to the ideal ear voltage should be determined.

In this paper, the effects of ear fields on a HIF pulse are studied using a fast-running envelope code CIRCE, which has been described elsewhere [1,2]. We first present an analytic expression for the ear fields and briefly indicate how they are calculated in CIRCE. The effects of applying ideal ear fields at widely spaced ear cells are then summarized, and the consequences of approximating the ear fields by FETs are discussed.

II. Ear Model

As discussed in Ref. [2], the beam longitudinal dynamics is modeled in CIRCE by treating slices of the beam as Lagrangian fluid elements. This approach implicitly assumes that the beam has a negligible longitudinal temperature and that the slices remain approximately collinear. An approximate β equation is obtained by retaining only the electrostatic force in the single-particle motion equations and averaging the axial component over the beam cross-section. For a beam in a straight lattice with an ion mass M and charge state q, we obtain

$$\frac{d\beta}{ds} = \frac{qe}{\beta M c^2} \left(E_{ext} + E_b \right). \tag{2}$$

Here, the average external electric field E_{ext} is approximated by the voltage across accelerating modules divided by the gap length, and the field due to the presence of the beam is found to be approximately

$$E_b \approx g \left[\frac{\partial}{\partial \tau} \left(\frac{I_b}{\beta^2 c^2} \right) + \frac{I_b}{\beta^2 c} \frac{d\beta}{ds} \right], \tag{3}$$

where R is the beam-pipe radius, and g is given by

$$g \approx \frac{1}{2\pi\epsilon_0} \ln \left(\frac{2R}{a+b} \right). \tag{4}$$

In deriving the beam field, the radial electrostatic field is assumed to vary over a much shorter scale length than E_b, and the continuity equation is used to convert derivatives with respect to s into τ derivatives. Combining Eqs. (2)

* The research was performed under the auspices of the U. S. Department of Energy by Lawrence Livermore National Laboratory under Contract No. W-7405-ENG-48.

a. Present address: Lawrence Berkeley Laboratory, Berkeley, CA

and (3), we obtain an equation for E_b in terms of E_{ext} and the time derivative of I_b/β^2c^2:

$$E_b \approx \frac{g}{1 - g\frac{I_b}{\beta^3}\frac{qe}{Mc^3}}\left[\frac{\partial}{\partial\tau}\left(\frac{I_b}{\beta^2c^2}\right) + \frac{I_b}{\beta^3}\frac{qe}{Mc^3}E_{ext}\right]. \quad (5)$$

The first term in Eq. (5) accounts for the beam space charge, while the second, usually much smaller, represents the induced electric field associated with beam acceleration and has no effect on the beam length. The ear field that balances the space charge force is then given by

$$E_{ear} \approx -\frac{g}{1 - g\frac{I_b}{\beta^3}\frac{qe}{Mc^3}}\frac{L_g}{2NL}\frac{\partial}{\partial\tau}\left(\frac{I_b}{\beta^2c^2}\right), \quad (6)$$

where we have inserted the previously mentioned gap-occupancy factor. Typically, the denominator in the leading factor of Eq. (6) may be approximated by unity, so the expression reduces to Eq. (1) in the limit of continuous acceleration.

For calculation, we use Eq. (6) to generate a table of ideal ear-field values on a fine time grid centered at the beam midpoint. Field values may be obtained by linear interpolation between tabulated values when modeling smoothly varying ear fields, or the values may be replaced by an appropriate stairstep waveform to model the field expected from FETs. For an even number of voltage steps $2N_s$, specified by the user, the size of field steps ΔE_z is chosen so that the maximum electric field excursion of the approximate waveform exceeds that of the ideal signal by about one step, ensuring that the beam ends are sufficiently confined. The timings of the field steps are tabulated by stepping through the ear-field values and calculating by linear interpolation the times at which the ideal field approximately equals $(n + \frac{1}{2})\Delta E_z$, for integer n. The stairstep waveform can then be constructed by increasing the electric field by ΔE_z at the tabulated step times. Alternately, either N_s separate waveforms with steps occuring in antisymmetric pairs or $2N_s$ waveforms with single steps can be generated to model FET switching without an inductive adder. This step algorithm clearly is appropriate only for ear fields that are monotone nondecreasing, but this constraint is normally satisfied for HIF beams.

III. Results

Since we are interested in effects of ear-cell spacing and waveform nonidealities, we choose here to model a straight lattice resembling that of a HIF driver but with none of the complications of a realistic design. The beam used in the calculations consists of singly charged 200 amu ions with an initial energy of 1 GeV, an initial duration of 0.750 μs, and a total charge of 90 μC, making the peak current about 132 A. The current is taken to be constant over the central 60% of the pulse, and the normalized emittance is taken to be 1×10^{-5} m-rad, making the beam strongly space-charge dominant. The lattice consists of 1.6 T quadrupole doublets with 30% occupancy and one accelerating cell per 2.9 m half-lattice period. The main differences between this model lattice and that for a linear HIF driver are that the 53 kV/m acceleration gradient is lower, the lattice parameters do not change with increasing beam energy, and there

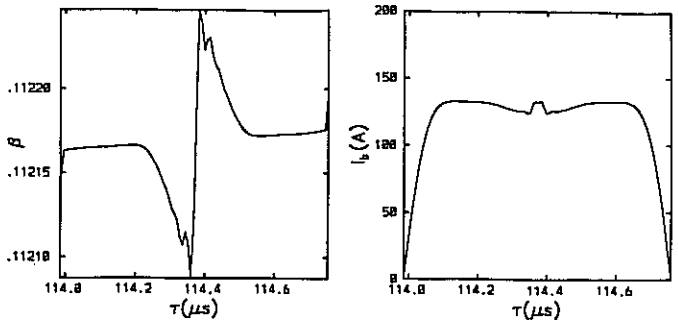

Fig. 1 Beam quantities as functions of arrival time τ for ideal voltage ears applied at every induction cell: (a) beam $\beta = v/c$; (b) beam current I_b.

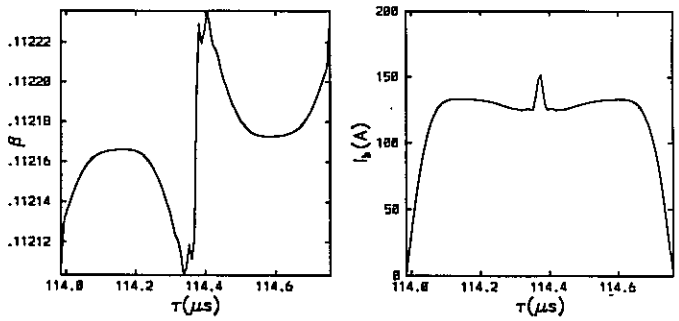

Fig. 2 Beam quantities as functions of τ for ideal field ears applied at one induction cells every 8 periods: (a) β; (b) I_b.

is no beam compression. Also, there are no magnet errors or initial mismatches.

When the pulse is accelerated for about 3.7 km through this lattice in the absence of ear fields, the beam space charge causes the beam to lengthen by a factor of 3.2 and develop a 2% velocity tilt from head to tail. In contrast, when an ear field calculated from Eq. (6) is added to the constant accelerating field in each induction cell, the beam duration remains constant within 2%, and variations in β along the beam are kept to about $\pm 0.05\%$. Plots of β and I_b as functions of the arrival time τ at the end of the lattice are shown in Fig. 1. The small ripple seen in I_b results from space-charge waves launched at the beam ends, and the pronounced β variation near the beam midpoint comes from the axial electric fields associated with the beam density ripple. Space-charge waves are iniated near the ends because the same ear field is used in all cells, whereas Eq. (6) indicates that the ear field should in fact decrease somewhat as β increases. The resulting ripples are found in longer CIRCE runs to produce progressively shorter-wavelength fluctuations due to interference, but in a real beam, we would expect to see the wave energy thermalize and increase the beam longitudinal emittance.

Increasing the spacing between ear cells in this lattice makes little change in longitudinal confinement. For the case shown in Fig. 2, with the ideal ear field applied in one induction cell every eight full periods, the change in length, amounting to about 0.4%, is too small to be visible. The

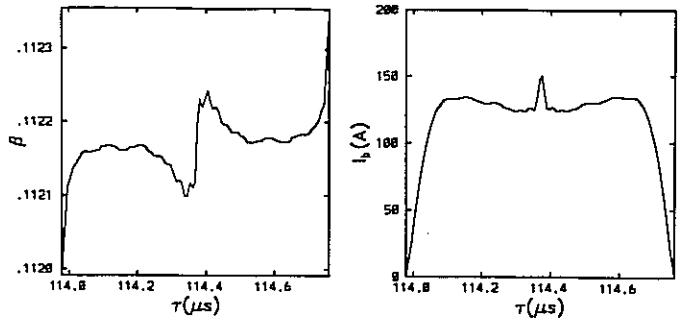

Fig. 3 Beam quantities as functions of τ for a 20-step approximation of ideal ears applied at one induction cell every 8 periods: (a) β; (b) I_b.

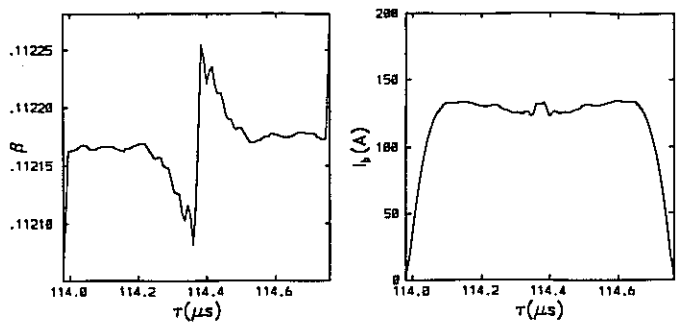

Fig. 4 Beam quantities as functions of τ for a 20-step approximation of ideal ears with pairs of antisymmetric steps applied in 10 successive induction cells every 8 periods: (a) β; (b) I_b.

most obvious consequence of the wider spacing in this case is the apparent overcompensation for space charge near the beam ends, which is due to the velocity kick imposed at the previous ear cell not having fully relaxed at the end of the lattice. In addition, there is a some initial fluctuation in the beam duration with s due to the more poorly matched ear fields and consequently somewhat enhanced generation of space-charge waves. These changes are exaggerated when the ear-cell spacing is increased to one ear cell per 16 lattice periods, but they still constitute minor changes of basically good longitudinal confinement. Apparently, longitudinal confinement remains effective and non-disruptive so long as the ear fields are applied frequently compared with the characteristic time for beam expansion.

The principal limit on the spacing of ear cells in these cases arrises from insulator breakdown in the induction cells. Current insulator technology limits electic fields to less than about 5×10^6 V/m, with certain exotic materials tolerating up to 10^7 V/m. For a given cell voltage, the electric field may be reduced by enlarging the gap, but this approach is limited by the increasing cell acceptance for wakefields, which enhances growth of the beam break-up instability. Balancing these limitations, reasonable values for the gap size lie in the range of 2 - 4 cm, and for the computational example, we use 3.5 cm. When the ear fields are imposed in every cell, the maximum ear-field magnitude for the example, occuring at the beam ends, is about 2.5×10^6 V/m, and when the ears are applied in one cell every eight periods, this maximum field amplitude increases to 4.0×10^7 V/m. Unless the beam-current rise and fall times are lengthened, which would reduce the driver efficiency, the ear fields must be applied in this case at least once every four periods to avoid breakdown. This constraint becomes progressively tighter as the beam is accelerated to 10 GeV due to the increasing compression and correspondingly shorter current rise times.

Approximating the ear field by a series of steps in effect introduces a small mismatch at the front and back of each step. Since the ions at the bottom of each step are accelerated less than the ions immediately behind them at the top of the step, an increase in beam density is expected near each step, resulting in low-amplitude space-charge waves. The simulations suggest that these waves are not seriously detrimental so long as five or more steps are used to approximate each ear, or ten to represent the full ear field. As an illustration, Fig. 3 shows the final β and I_b as functions of τ for a case using ten-steps per ear and one ear-cell every eight periods. When the plots are compared with Fig. 2, the principal difference is the addition of high-frequency ripple to both quantities. For this case, as well as for the case with five steps per ear, thermalization of this ripple would make a small contribution to the expected longitudinal emittance. However, when fewer than five steps are used to approximate each ear, the amplitude of space-charge waves increases substantially and is clearly unacceptable for three steps per ear.

The effect of imposing field steps in different cells is illustrated in Fig. 4. The beam and fields used for that figure are identical to those in Fig. 3 except that field steps are imposed in antisymmetric pairs in the acceleration cells of five successive lattice periods, with the field pattern being repeated every eight periods. Comparing Figs. 3 and 4, we see that the level of short-wavelength variations in β and I_b is somewhat reduced, and the incomplete relaxation of β at the head and tail is effectively eliminated. This later effect is expected, because the beam ends receive a series of small kicks rather than infrequent large kicks and therefore are never displaced far from equilibrium. The order that the field steps are applied appears to be unimportant. Reversing or scrambling the order that the pairs of steps are applied changes the details of the short-wavelength variations but not their average amplitude, and applying the field steps singly rather than in pairs is likewise found to make a negligible difference. Besides being somewhat less disruptive, this approach of applying the ear-field steps in separate cells has the obvious advantage of reducing the field stress in any cell and thereby avoiding breakdown. In a HIF driver using induction cells, distributed ears of this sort are likely to be the only practical method for longitudinal confinement of the beam.

References

[1] W. M. Sharp, J. J. Barnard, and S. S. Yu, "Envelope Model of a Heavy-Ion Recirculator," *Part. Accel.*, **37-38**, 205 (1992).

[2] W. M. Sharp, J. J. Barnard, and S. S. Yu, "Transport and Error Sensitivity in a Heavy-Ion Recirculator," in *Proceeding of the 1991 IEEE Part. Accel. Conf* (IEEE, New Jersey, 1991), p. 260.